

Engineering Simulation of Lead–Acid Cell Characteristics and Processes in Batteries

V. Esfahanian Associate Professor evahid@ut.ac.ir	F. Torabi Ph. D. Candidate ftorabi@ut.ac.ir	R. Afzali VFERI Researcher
Vehicle, Fuel and Environment Research Institute Mechanical Engineering Department – University of Tehran		

Abstract

Predicting transient behavior of lead–acid batteries during charge and discharge process is a very important factor in many applications including Hybrid Electric Vehicles (HEV). In this paper, an engineering model based on fundamental chemical and electrochemical relations of lead–acid batteries is introduced. This model is capable to predict transient behavior of lead–acid batteries including charge and discharge cycles. It is also capable to predict acid consumption, SoC and porosity variation of electrodes as well. Since the model is based on electrochemical relations, it gives a good physical understanding of lead–acid phenomena. This model is verified with experimental tests and CFD codes. The results show that the developed model has a good accuracy within a very short time.

<i>a</i> Coefficient <i>A</i> Specific electroactive area, [cm ² /cm ³] <i>c</i> Acid concentration, [mol/cm ³] <i>e</i> Electric charge of electrone, 1.6×10^{-19} [C] <i>ex</i> Exponent in the effective property <i>E</i> Battery voltage [V] <i>E_{oc}</i> Open circute voltage [V] <i>F</i> Faraday constant, 96,487, [C/mol] <i>i₀</i> Transfer current density, [A/cm ²] <i>I</i> Current, [A] <i>j</i> Applied current density, [A/cm ²] <i>k</i> Conductivity of liquid, [S/cm] <i>MW</i> Molecular weight, g/mol	<i>N</i> Number of electrone <i>N_a</i> Avogadro number <i>N</i> Mole of acid [mol] <i>q</i> Electric charge [C] <i>Q</i> Electrode charge per volume [C/cm ³] <i>R</i> Universal gas constant, 8.314 [J/mol · K] <i>R_b</i> Battery ohmic resistance [Ω] <i>t</i> Time, [sec] <i>T</i> Temprature [K] <i>V</i> Electrolyte volume [cm ³] <i>x</i> Electrode thickness [cm] <i>y</i> Electrode height [cm] <i>z</i> Electrode width [cm]
Greek	
<i>ε</i> Porosity <i>φ</i> Electric potential [V] <i>α</i> Transfer coefficient for the electrode <i>ξ</i> Exponents for the specific active area	<i>σ</i> Conductivity of solid matrix [S/cm] <i>γ</i> Exponent for the exchange current density <i>ρ</i> Density of species

Subscripts/Superscripts

<i>eff</i> Effective, corrected for tortuosity <i>o</i> Initial value	<i>l</i> Liquid solution <i>s</i> Solid phase
--	--

1 Introduction

Predicting transient behavior of lead–acid batteries during charge and discharge process is a very important factor in many applications including Hybrid Electric Vehicles (HEV). Since HEV modeling requires a real–time modeling, an accurate and fast battery model is very crucial. Therefore, many researches are performing to find a suitable real–time model of batteries. The most practical way of modeling is based on equivalent circuit and computational fluid dynamics known as CFD [1, 2].

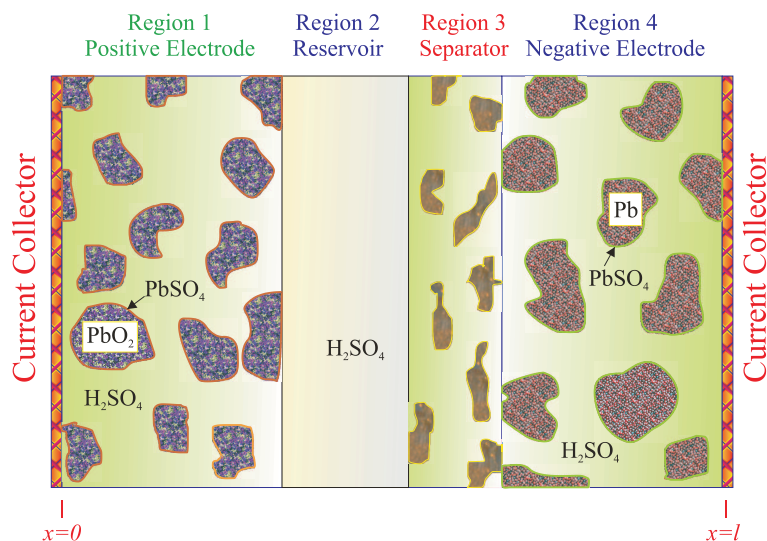


Figure 1: A typical model of lead–acid cell.

In equivalent circuit modeling, each phenomena in battery is modeled with an electrical element and the whole battery is modeled with an electrical circuit. Although this model is fast enough, but it contains a lot of simplification assumptions and many physical properties of the battery is ignored. On the other hand, this modeling needs a lot of experimental tests to obtain necessary parameters of the electrical elements [3].

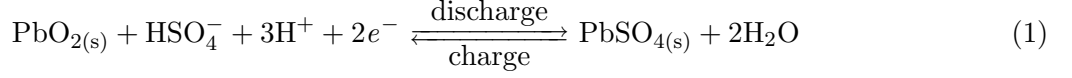
In CFD models governing transport equations are solved numerically using advanced CFD techniques and therefore it is very accurate and gives a deep understanding of involved physical phenomena [4]–[11]. But, this kind of modeling is normally time consuming, requires a lot of computer resources and thus is not suitable for real–time simulations.

In this paper, an engineering model based on fundamental chemical and electrochemical relations of lead–acid batteries is introduced. This relations can be found in many electrochemical books and handbooks [12]–[17]. This model is capable to predict transient behavior of lead–acid batteries including charge and discharge cycles. It is also capable to predict acid consumption, SoC and porosity variation of electrodes as well. Since the model is based on electrochemical relations, it gives a good physical understanding of lead–acid phenomena. On the other hand, in this model only simple algebraic relations is used and hence it is very fast which can be used in real–time simulations. This model is verified with experimental tests and CFD codes. The results show that the developed model has a very good accuracy within reasonable execution time.

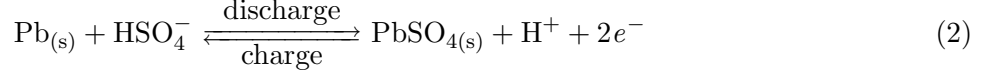
2 Mathematical Model

A typical lead–acid cell is shown schematically in Figure 1 which consists of the following regions: a lead–grid collector at $x = 0$ which is at the center of the positive electrode; a positive PbO_2 electrode; electrolyte reservoir; a porous separator; a negative Pb electrode; and finally, a lead–grid collector at $x = l$ which is at the center of the negative electrode. The positive and negative electrodes consist of porous solid matrices whose pores are flooded by a binary sulfuric acid, H_2SO_4 . Neglecting side reactions (like oxygen evolution in VRLA batteries), during charge and discharge, the following electrochemical reactions occur in the positive and negative electrodes

PbO₂ electrode:



Pb electrode:



2.1 Acid Concentration

Assume that the battery cell is charged (discharged) at the rate of I A. In this case, in an ideal situation, the transferred charge can be expressed as:

$$q = I \cdot \Delta t \quad (3)$$

The transferred charge can also be calculated from the following equation:

$$q = N \cdot e \quad (4)$$

in which e is the electrical charge of one electron and N is the number of transferred electrons. From equations (3) and (4), total number of transferred electrons can be obtained; i.e.:

$$N = \frac{q}{e} \quad (5)$$

The number of reacted mole can be found by dividing the number of transferred electrons to Avogadro's number ($N_a = 6.02 \times 10^{23}$):

$$\mathcal{N} = \frac{N}{N_a} \quad (6)$$

According to equations (1) and (2), the charge number is $n = 2$ which means that transfer of each two moles of electron is equal to consumption of two mole sulfuric acid. Therefore, the acid consumption can be easily calculated. On the other hand, since the initial acid concentration is known, the bulk acid concentration in each time can be found as follows:

$$\delta c = \frac{\mathcal{N}}{V_{\text{Electrolyte}}} \quad (7)$$

and finally, the acid concentration can be calculated by the following relation:

$$c^{n+1} = c^n - \delta c \quad (8)$$

in which superscripts n and $n + 1$ describe the time level.

2.2 Cell Voltage

When a battery is attached to an external current, I , the cell voltage can be calculated from [14]:

$$E = E_{oc} \pm [(\eta_{ct})_a + (\eta_c)_a] \pm [(\eta_{ct})_c + (\eta_c)_c] - IR_i \quad (9)$$

in which, E_{oc} is the open circuit voltage, $(\eta_{ct})_a$ and $(\eta_{ct})_c$ are activation polarization or charge-transfer overvoltage at anode and cathode. $(\eta_c)_a$ and $(\eta_c)_c$ are concentration polarization at anode and cathode, R_i is the internal cell resistance and I is the current passing through the cell. In this equation, $(-)$ and $(+)$ signs represent discharge and charge, respectively. From the above equation, it is obvious

that to obtain the variation of cell voltage during charge and discharge, the variations of open circuit voltage, overpotentials and internal resistance are required. Since in this model acid concentration assumed to be uniform, there would not be any acid concentration gradient and hence, concentration polarizations are zero.

In general, open circuit voltage is a function of acid concentration. This relation is tabulated in battery handbooks (i.e. [12]) which can be curve fitted to the following relation:

$$E_{oc} = - 6.742 \times 10^{18}c^8 + 2.112 \times 10^{17}c^7 - 2.761 \times 10^{15}c^6 + 1.973 \times 10^{13}c^5 - 8.307 \times 10^{10}c^4 + 2.111 \times 10^8c^3 - 3.182 \times 10^5c^2 + 3.170 \times 10^8c + 1.736 \quad (10)$$

Overpotential η_{ac} can be evaluated from Butler–Volmer equation [13]

$$j = i_o \left(\frac{c}{c_{ref}} \right)^\gamma \left\{ \exp \left(\frac{\alpha_a F}{RT} \eta_{ct} \right) - \exp \left(\frac{-\alpha_c F}{RT} \eta_{ct} \right) \right\} \quad (11)$$

in which j is transfer current density. The transfer current density, on the other hand, can be calculated from:

$$j = \frac{I}{A[(1 - \varepsilon)xyz]} \quad (12)$$

in which A is active area of electrode per volume of active material and $(1 - \varepsilon)xyz$ is active material volume in each time. Active area is one of the most important factors in battery modeling. This factor is a function of porosity and shape of the electrode morphology. This relation can be modeled as [10]:

$$A = A_{max}SoC^\xi \quad \text{for Discharge} \quad (13)$$

$$A = A_{max}(1 - SoC^\xi) \quad \text{for Charge} \quad (14)$$

in which ξ relates the dependency of active area to morphology factor and is considered $\xi = 0.55$ in this study. Equations (8), (11) and (12) can be used to obtain overpotential.

2.3 State of Charge (SoC)

State of Charge of battery can be simply obtained by the following relation:

$$SoC^{n+1} = SoC^n \pm \frac{1}{(1 - \varepsilon)xyz} \frac{\int Idt}{Q_{max}} \quad (15)$$

in which superscripts n and $n + 1$ describe the time level, and also (+) and (−) signs refer to charge and discharge, respectively. Q_{max} is the maximum theoretical charge of the electrode [10].

2.4 Electrode Porosity

During charge and discharge, lead sulfate converts to lead and lead–dioxide and vice versa. Because of this conversion, porosity of electrodes changes as a function of time. Since this parameter has a crucial role in battery performance, it should be modeled. Variation of porosity can be modeled as follows [10]:

$$\frac{d\varepsilon}{dt} - a \frac{Aj}{2F} = 0 \quad (16)$$

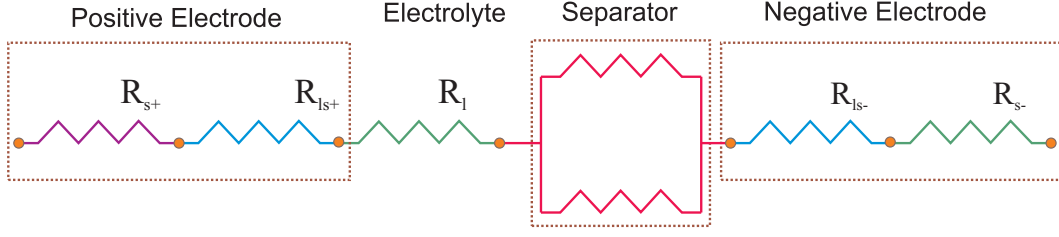


Figure 2: Resistance model of lead–acid cell.

in which

$$a = \left(\frac{MW_{\text{PbSO}_4}}{\rho_{\text{PbSO}_4}} - \frac{MW_{\text{PbO}_2}}{\rho_{\text{PbO}_2}} \right)$$

for positive electrode and

$$a = \left(\frac{MW_{\text{Pb}}}{\rho_{\text{Pb}}} - \frac{MW_{\text{PbSO}_4}}{\rho_{\text{PbSO}_4}} \right)$$

for negative electrode.

2.5 Cell Resistance

Another parameter that affects the battery voltage is cell or battery resistance (eq. (9)). In this model, it is assumed that acid concentration is uniform across the cell, thus there is not any acid gradient in battery model. This assumption results that concentration polarizations in equation (9) (i.e. $(\eta_c)_a$ and $(\eta_c)_c$) are neglected in this model.

Electrical resistance of the cell consists of the resistance of positive and negative electrodes, electrolyte and separator. These resistance are illustrated in Figure 2, schematically.

Resistance of solid electrode can be calculated by the general known formula of resistance as follow:

$$R_b = \frac{d}{\sigma^{\text{eff}} A} \quad (17)$$

in which d , σ^{eff} and A are width, equivalent electrical conductivity and nominal cross section of electrode respectively. Since electrodes of lead–acid batteries are porous, effective physical properties should be considered. In this paper, the effective properties can be obtained by following relation:

$$\psi^{\text{eff}} = \psi(1 - \varepsilon)^{\text{ex}} \quad (18)$$

in which superscript ex is should be obtained from experiment and in this study is taken as 1.5.

Resistance of electrolyte can be obtained in a similar manner:

$$R_l = \frac{x}{k^{\text{eff}} A_{\text{eff}}} \quad (19)$$

in which k^{eff} is effective electrolyte conductivity.

Resistance of separator can be considered as two parallel resistance. One is the resistance of electrolyte inside of separator which can be calculated with equation (19). The second resistance is the resistance of the separator itself which can be calculated as follow:

$$R_s = \frac{x_s}{\sigma_s A_{\text{eff}}} \quad (20)$$

in which σ_s is the resistance of separator material. By calculating all the mentioned resistances, the overall resistance of the cell can be calculated.

3 Summary

In summary, equations (8), (9), (15) and (16) are used to calculate four main parameter of a lead–acid battery namely, acid concentration, cell voltage, SoC and electrode porosity. The flowchart of this calculation is shown in Figure 3. To verify the present model, three different battery cell is selected. The characteristics of these cells are given in Table 1. Cell I is first presented by Gu et al. [5] and reconsidered by Gu et al. [10]. All necessary information can be found in [10, 11]. Cell II was first solved by CFD method by Gu et al. [11] and is also reproduced by Gu et al. [10] and Esfahanian & Torabi [2]. In this cell, all the three phenomena (i.e. discharge, rest and charge) were simulated numerically. The necessary information can be found in [11, 10, 2]. Cell III was introduced by Nguyen et al. [4] to predict the effect of separator design which is considered as the third sample for verifying the present model.

4 Results and Discussions

1. Cell I

Cell I is selected to investigate discharge process of battery cells. This cell is subjected to two different current namely $I = -10 \text{ mA/cm}^2$ and $I = -40 \text{ mA/cm}^2$. Figure 4 shows the variation of cell I voltage versus time. These simulations are compared by numerical and experimental results of other scientists. As it can be seen, the results of this electrochemical modeling show a very good agreement with other modelings and this model is capable to accurately model both discharge and charge process.

2. Cell II

Cell II is selected to investigate both discharge and charge process of battery cells. This cell is subjected to a high applied current density of $I = -340 \text{ mA/cm}^2$ for discharge. Figure 5 shows the variation of cell II voltage versus time. The results show that this model can predict discharge of the cell very accurately at -18°C but there is a small deviation at $+25^\circ\text{C}$. The main cause of this deviation is that the present model calculations are based on bulk properties at each time step. Therefore, when the physical processes have a very high spatial gradient, this model shows some deviation. As it can be seen in Figure 5 (b), in charge process, this model shows a good agreement with other simulations. This is because the charge process is performed with a fairly low applied current density (i.e. $I = +20 \text{ mA/cm}^2$).

Figure 6 shows the variation of bulk acid concentration vs. time. This figure shows that this model accurately simulates acid consumption. It should be noted that CFD models are able to solve acid concentration distribution. Since the present model captures only the bulk acid concentration, to compare it with CFD results, distributed acid concentration of CFD models has been integrated over the cell width to obtain bulk values. As it can be seen in this figure, the consumption of sulfuric acid has a nearly linear behavior.

Figure 7 shows the variation of electrode porosity vs. time. As it was mentioned, to compare present results with CFD models, electrode porosity of CFD models has been integrated to obtain a mean value. Since electrode porosity variation is highly nonlinear and depends on many parameters (and also the applied current density is very high), the results of this model has slightly deviation from CFD model. But in general, it shows nearly the same behavior.

Figure 8 shows the variation of SoC vs. time which is compared with mean value of the CFD model. As it can be seen, in both working temperatures, the deviation of this model and CFD

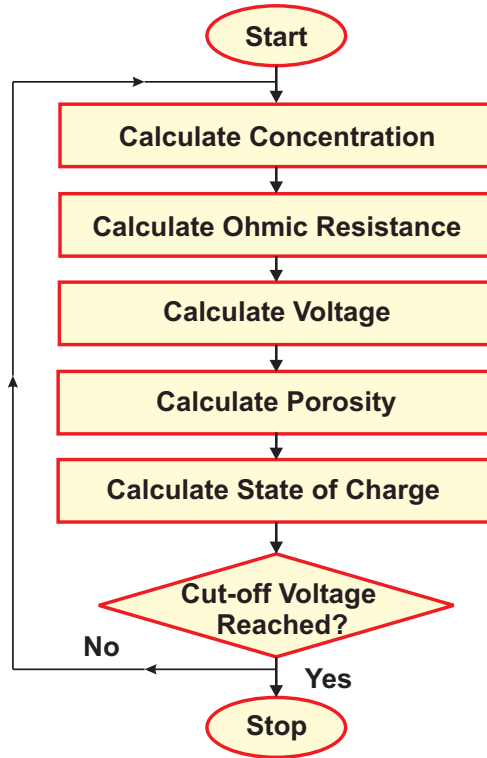


Figure 3: Flowchart of the present model.

is less than 10%. This shows that this model is able to predict SoC of the cell within good accuracy of engineering expectations.

3. Cell III

Cell III consists of a GMAT separator, and hence does not have an electrolyte region. This case was first modeled by H. Gu et al. [4] and is modeled by the present approach. As it can be seen in Figure 9, variation of voltage and acid concentration is accurately simulated using the present model.

In all above cases, this model is also very fast comparing to CFD models. For example a typical discharge simulation of cell II needs about 30 sec of CPU time while the present model requires much less than 1 sec. This shows the capability of the present model for real-time simulations which is very crucial in HEV simulators and also monitoring apparatus.

5 Conclusions

In this paper, an accurate, simple and fast model based on electrochemical relations is introduced. This model is capable to predict variation of voltage, acid consumption, SoC and porosity of electrodes very fast and accurately. Although in this model only simple algebraic relations are used, it is accurate enough to predict many battery characteristics from engineering point of view. This model can be used for preliminary design of batteries. The accuracy of this model was verified with three different selected cells. The results show that in addition to its simplicity, this model is accurate enough.

Table 1: Simulated values of the samples.

	Cell I	Cell II	Cell III
Cell Dimensions [cm]			
• Height	8	8	13.9
• Width	4	4	10.7
Thickness [cm]			
• Positive Electrode	0.0865	0.06	0.08
• Electrolyte	0.16	0.055	-
• Separator	0.056	0.014	0.1
• Negative Electrode	0.0815	0.06	0.09
Porosity (ε)			
• Positive Electrode	0.55	0.53	0.62
• Separator	0.6	0.73	0.912
• Negative Electrode	0.61	0.53	0.6
Exchange Current Density [mA/cm ²]			
• Positive Electrode	6×10^{-4}	10	3.19×10^{-8}
• Negative Electrode	8×10^{-3}	10	4.96×10^{-7}
Maximum Charge [C/cm ³]			
• Positive Electrode	2800	5660	2620
• Negative Electrode	2471	5660	3120
Maximum Active Area [cm ² /cm ³]			
• Positive Electrode	20.5×10^4	100	3.3×10^5
• Negative Electrode	2.5×10^4	100	2.3×10^4
Operating Conditions			
• Applied Current Density [mA/cm ²]	-10 & -40	-340 & +20	-408
• Operating Temperature [°C]	21.7	25 & -18	-18

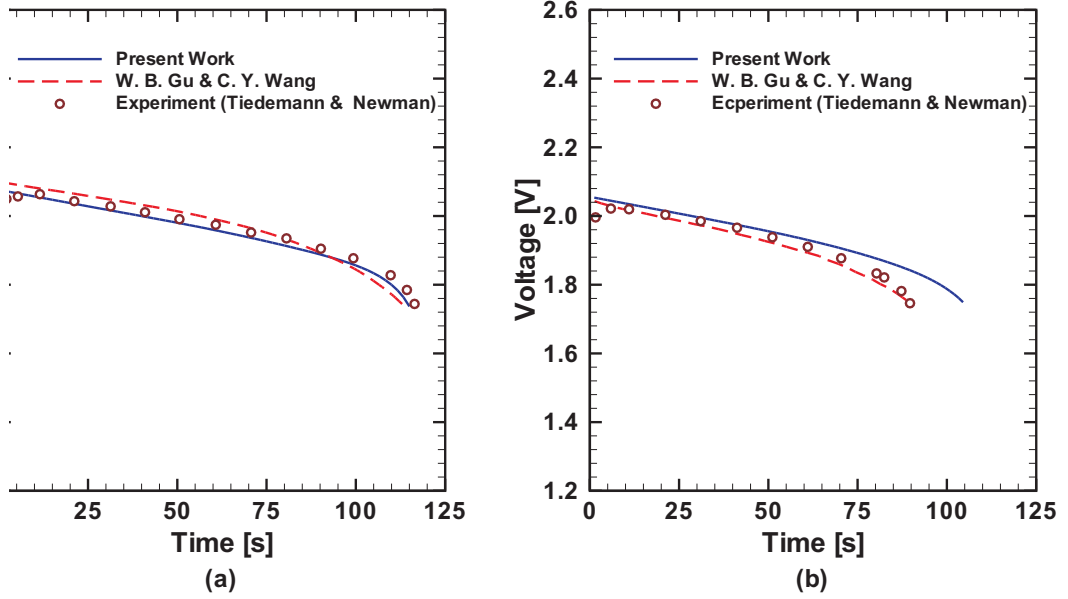


Figure 4: Variation of cell voltage vs. time of cell I at (a) $I = -10 \text{ mA/cm}^2$ and (b) $I = -40 \text{ mA/cm}^2$.

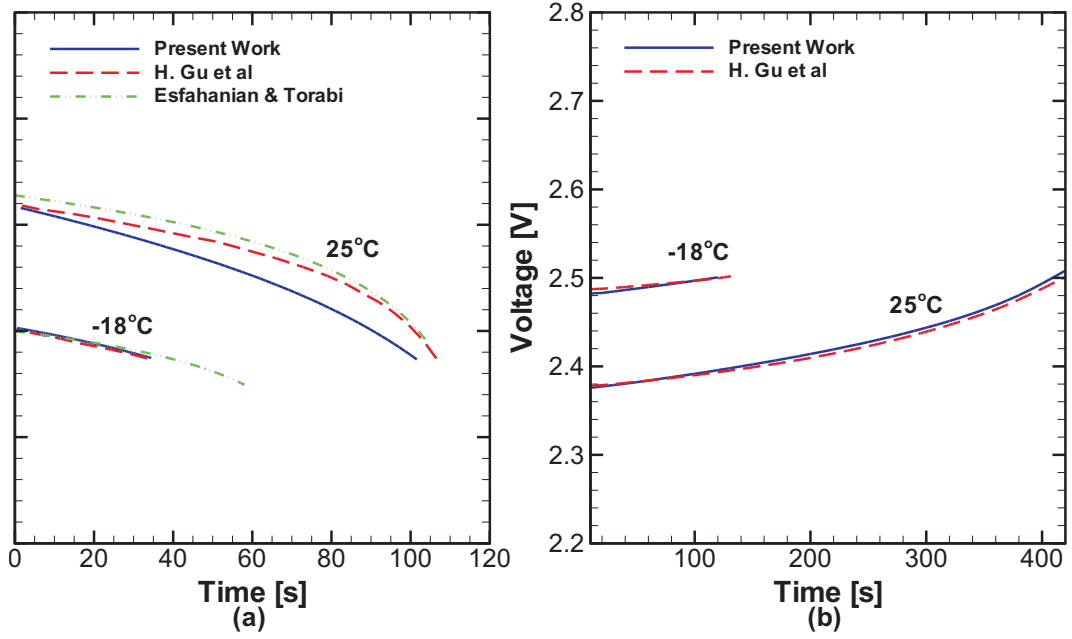


Figure 5: Variation of cell voltage vs. time of cell II at (a) Discharge and (b) Charge.

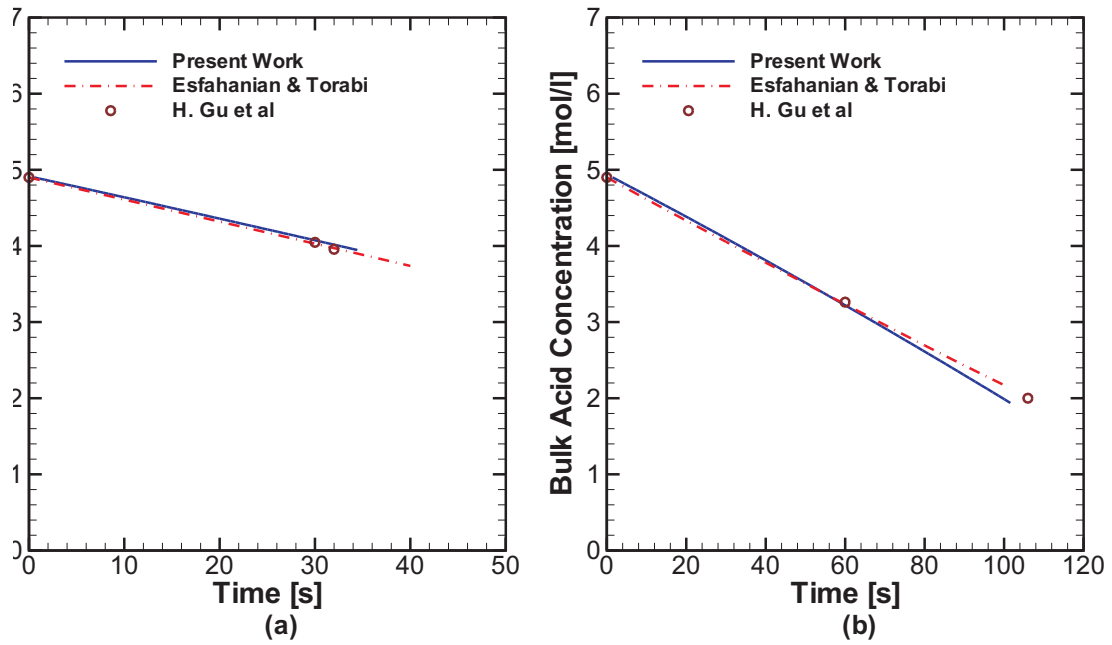


Figure 6: Variation of bulk acid concentration vs. time at (a) $T = -18\text{ }^{\circ}\text{C}$ and (b) $T = +25\text{ }^{\circ}\text{C}$.

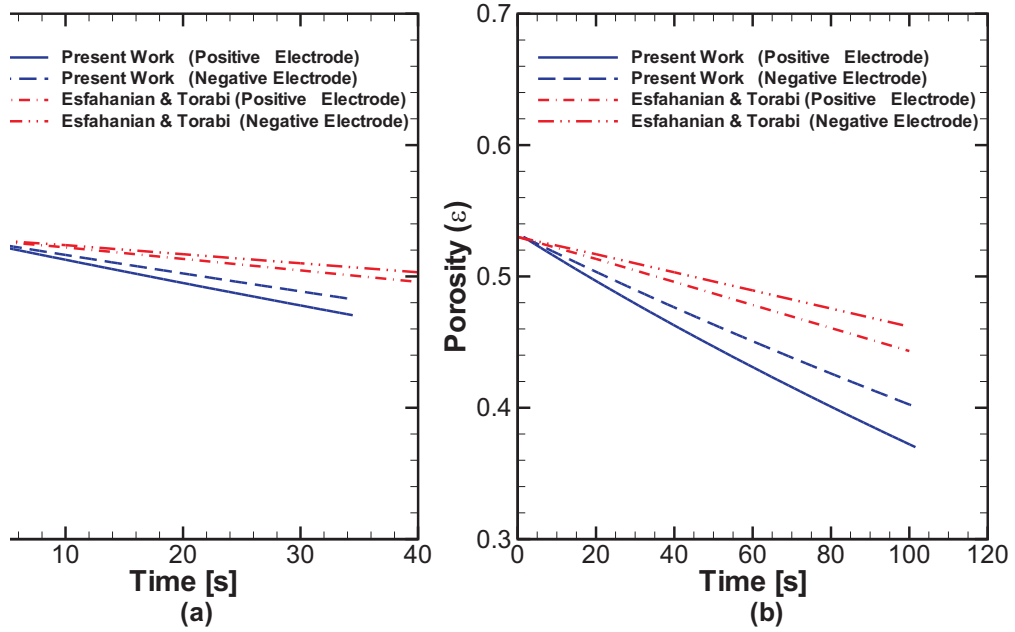


Figure 7: Variation of electrode porosity of cell II vs. time at (a) $T = -18\text{ }^{\circ}\text{C}$ and (b) $T = +25\text{ }^{\circ}\text{C}$.

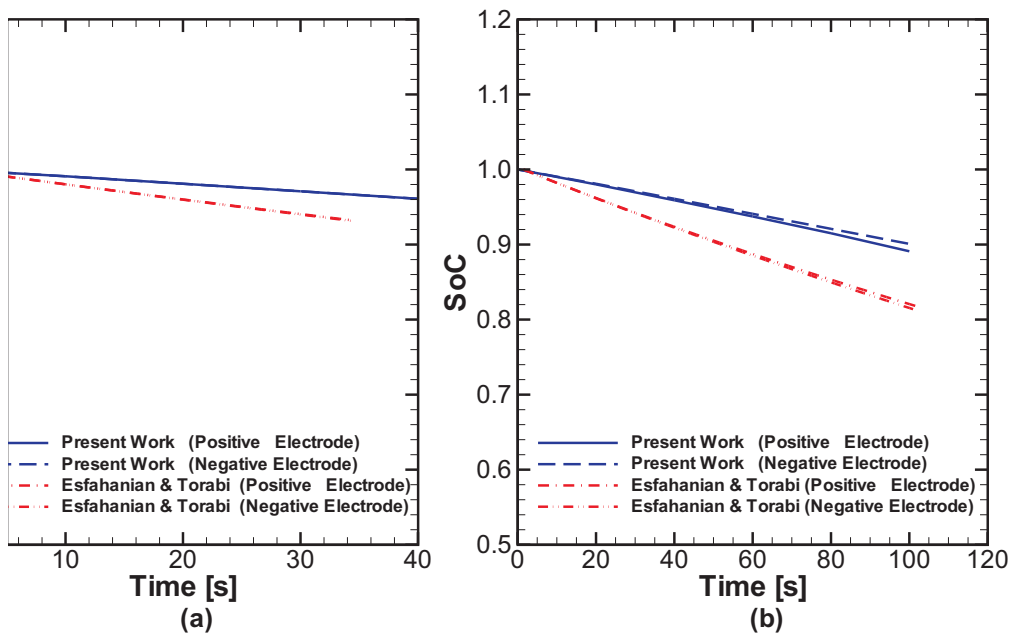


Figure 8: Variation of SoC of cell II vs. time at (a) $T = -18\text{ }^{\circ}\text{C}$ and (b) $T = +25\text{ }^{\circ}\text{C}$.

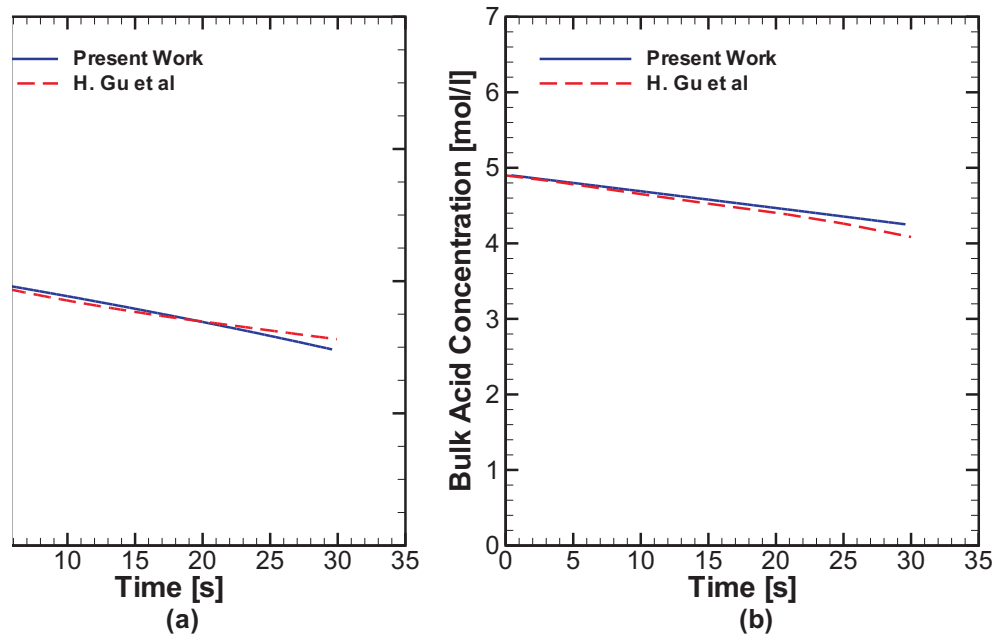


Figure 9: Variation of (a) cell voltage and (b) acid concentration vs. time of cell III.

6 Acknowledgments

The authors wish to gratefully acknowledge the financial support from Niru Battery Manufacturing Co. and Vehicle, Fuel and Environment Research Institute of University of Tehran.

References

- [1] V. Esfahanian, F. Torabi, “Numerical Simulation of Lead–Acid Batteries using Keller-Box Method,” Presented in LABAT’05 Bulgaria, 2005.
- [2] V. Esfahanian, F. Torabi, “Numerical Simulation of Lead–Acid Batteries using Keller-Box Method,” *J. Power Sources*, 158 (2006) 949–952.
- [3] N. A. Monfared, N. Gharib, H. Moqtaderi, M. Hejabi, M. Amiri, F. Torabi, A. Mosahebi, “Prediction of state–of–charge effects on lead–acid battery characteristics using neural network parameter modifier,” *J. Power Sources*, 158 (2006) 932–935.
- [4] T. V. Nguyen, R. E. White and H. Gu, “The effect of Separator Design on the Discharge Performance of a Starved Lead–Acid Cell”, *J. Electrochem. Soc.* 137, 2998, 1990.
- [5] T. V. Nguyen, R. E. White, “A mathematical model of a hermetically sealed lead–acid cell,” *Electrochim. Acta*, 38, 935, 1993.
- [6] D. M. Bernardi, M. K. Carpenter. “A Mathematical Model of the Oxygen–Recombination Lead–Acid Cell,” *J. Electrochem. Soc.* 142 (1995) 2631–2642.
- [7] C. Y. Wang, W. B. Gu, “Micro-Macroscopic Coupled Modeling of Batteries and Fuel Cells: I Model development,” *J. Electrochem. Soc.* 145 (10) (1998) 3407-3417.

- [8] C. Y. Wang, W. B. Gu, "Micro-Macroscopic Coupled Modeling of Batteries and Fuel Cells: II Application to Nickel–Cadmium and Nickel–Metal Hydride Cells," *J. Electrochem. Soc.* 145 (10) (1998) 3418-3427.
- [9] W. B. Gu, G. Q. Wang, C. Y. Wang, "Modeling the overcharge process of VRLA batteries," *J. Power Sources*, 108 (2002) 174–184.
- [10] H. Gu, C. Y. Wang, B. Y. Liaw, "Numerical modeling of coupled electrochemical and transport processes in lead acid cell," *J. Electrochem. Soc.* 144 (6) (1997) 2053-2061.
- [11] H. Gu, T. V. Nguyen, R. E. White, "A mathematical model of a lead-acid cell: discharge, rest and charge," *J. Electrochem. Soc.* 134 1987 2953.
- [12] D. Berndt, *Maintenance-Free Batteries*, 2nd Edition, John Wiley & Sons Inc., Research Studies Press Ltd., 1997.
- [13] J. Newman, *Electrochemical Systems*, 3rd Edition, John Wiley & Sons Inc., Hoboken, NJ 2004.
- [14] D. Linden, T. B. Reddy, *Handbook of Batteries*, 3rd Edition, McGraw–Hill Inc., 2002.
- [15] A. J. Bard, L. R. Faulkner, *Electrochemical Methods*, John Wiley & Sons Inc., 2001.
- [16] T. R. Crompton, *Battery Reference Book*, 2nd Edition, Butterworth–Heinemann Ltd., 1995.
- [17] H. Bode, *Lead–Acid Batteries*, John Wiley and Sons, New York, 1977.